

# A Novel 0.3-0.31 THz GaAs-Based Transceiver with On-Chip Slotted Metamaterial Antenna Based on SIW Technology

Mohammad Alibakhshikenari<sup>1\*</sup>, Bal S. Virdee<sup>2</sup>, Chan H. See<sup>3,4</sup>, Raed Abd-Alhameed<sup>5</sup>, Francisco Falcone<sup>6</sup>, and Ernesto Limiti<sup>1</sup>

<sup>1</sup> Electronic Engineering Department, University of Rome “Tor Vergata”, Via del Politecnico 1, 00133, Rome, ITALY

<sup>2</sup> London Metropolitan University, Center for Communications Technology, London N7 8DB, UK

<sup>3</sup> School of Engineering and the Built Environment, Edinburgh Napier University, 10 Colinton Road, Edinburgh, EH10 5DT, UK

<sup>4</sup> School of Engineering, University of Bolton, Deane Road, Bolton, BL3 5AB, UK

<sup>5</sup> School of Electrical Engineering & Computer Science, University of Bradford, Bradford, BD7 1DP, UK

<sup>6</sup> Electric and Electronic Engineering Department, Universidad Pública de Navarra, SPAIN

\* alibakhshikenari@ing.uniroma2.it

**Abstract:** This paper presents a novel on-chip antenna with fully integrated 0.3-0.31 THz transceiver implemented on 0.5 $\mu$ m GaAs substrate. The transceiver consists of a voltage-controlled oscillator (VCO), a buffer, a modulator, a power amplifier, a frequency tripler, and an on-chip antenna. The proposed on-chip antenna design is based on metamaterial (MTM) slots and substrate integrated waveguide (SIW) technologies. The SIW antenna operates as a high-pass filter and an on-chip radiator to suppress the unwanted harmonics and radiate the desired signal, respectively. Dimensions of the on-chip antenna is 2 $\times$ 1 $\times$ 0.0006 mm<sup>3</sup>. The average radiation gain and efficiency of proposed on-chip antenna is >1.0 dBi and ~55%, respectively. The transceiver provides an average output power of -15 dBm over 0.3-0.31 THz, which is suitable for near-field active imaging applications at terahertz region.

**Keywords:** On-chip antenna, metamaterial, terahertz (THz), substrate integrated waveguide (SIW), transceiver, Gallium Arsenide (GaAs) substrate, longitudinal and transverse slot arrays.

## I. INTRODUCTION

High frequencies technologies in the millimetre-wave and terahertz bands have been successfully employed in safety and biomedical applications, non-destructive detection, and non-ionizing cancer imaging [1, 2]. Such systems are based on III-V technology [3] or require quasi-optical functional blocks [4], which is undesirable as they are physically large and uneconomic. Recent advances in CMOS FETs and SiGe HBTs with significantly increased  $f_T$  and  $f_{max}$  have resulted in the realization of monolithic transmitters and receivers operating at millimetre-wave [5] and terahertz (THz) bands [6-8].

In this paper, an investigation is presented of a fully integrated on-chip antenna designed on GaAs based transceiver. The metamaterial slotted on-chip antenna is implemented on a SIW [9, 10] for integration within 300-310 GHz transceiver to efficiently radiate the desired signal and suppress the unwanted harmonics. In the architecture of the transceiver, a frequency tripler with

SIW slotted metamaterial on-chip antenna has conjugately matched to improve the performance and reduce mismatching.

## II. TRANSCEIVER CIRCUIT DESIGN

### A. Block Diagram

The block diagram of the proposed THz transceiver shown in Fig. 1 consists of a voltage-controlled oscillator (VCO), a buffer, a modulator, a power amplifier, a frequency tripler, and an on-chip antenna. The frequency tripler based architecture is used to achieve terahertz operation using the 0.5 $\mu$ m GaAs with  $f_T$  and  $f_{max}$  of 150 GHz and 220 GHz, respectively. A switch-based modulator implemented in 0.5 $\mu$ m MOSFET is included in this transceiver to enhance its functionality for potential applications including high-accuracy ranging and ultra-high data-rate (~10 Gbps) wireless communication. The modulation function is disabled for the Fourier-transform infrared spectroscopy (FTIR) measurement.

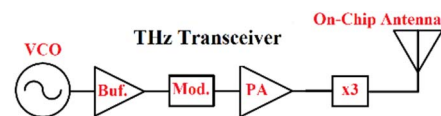


Fig. 1. Block diagram of the fully integrated terahertz transceiver with an on-chip SIW antenna.

### B. Voltage-Controlled Oscillator (VCO)

Schematic of the push-push cross-coupled VCO is shown in Fig. 2. The VCO's resonant frequency is controlled by inductor ( $L$ ) and varactor ( $C_V$ ). The varactor ( $C_V$ ) is realized by connecting the emitter and the base of an HBT transistor and using the reverse biased collector-base junction. Overall capacitance is the sum of the collector-base junction capacitance and collector-substrate parasitic capacitance. One quarter-wavelength microstrip line ( $TL_1$ ) at 150 GHz is placed at the coupled node of the HBTs ( $Q_1$  and  $Q_2$ ) to extract the second harmonic signal, which provides high impedance for the output signal and dc path for resonator.

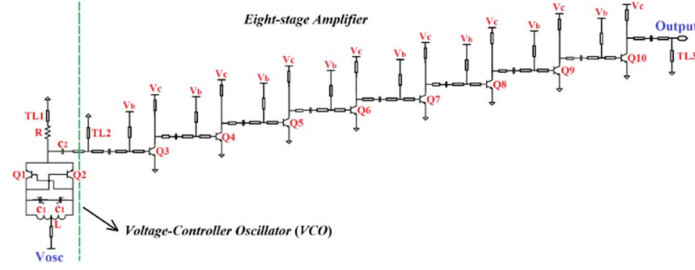


Fig.2. Circuit schematic of the voltage-controller oscillator (VCO) and the eight-stage amplifier.

### C. Buffer and Power Amplifier

Fig.2 shows the schematic of an eight-stage common-emitter configuration used for buffering and power amplification. To minimise parasitic effect and the chip size the biasing network is combined with the matching network. To guarantee the stability of whole amplifier, each stage of amplifier has been designed to be unconditionally stable over the frequency range of interest.

### D. Frequency Tripler ( $\times 3$ )

Circuit schematic of the frequency tripler is shown in Fig.3. The frequency tripler is based on the nonlinear characteristics of two cascoded HBTs ( $Q_1$  and  $Q_2$ ). In conventional designs a bandpass filter is used to eliminate the unwanted fundamental and harmonic products at the output. At such high frequencies a bandpass filter is challenging to realise for low insertion-loss and compact chip size. Hence, we have adapted an open-stub  $TL_1$  at  $2f_0$  to suppress all even-harmonics. The LC network ( $TL_2$  and  $C_1$ ), which doubles for DC biasing, is employed here to reject the fundamental signal ( $f_0$ ) and pass the desired  $3f_0$  signal.

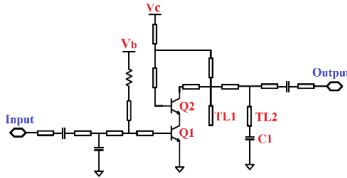


Fig.3. Circuit schematic of the frequency tripler.

Internal matching is used in integration of the frequency tripler and the on-chip SIW antenna. These two components are conjugate matched to reduce the size and improve the conversion gain. The simulated time-domain waveforms of the designed frequency tripler are plotted in Fig.4. It is evident that the  $3^{\text{rd}}$  harmonic ( $3f_0$ ) is generated with dominating amplitude. The fundamental signal ( $f_0$ ) is also shown. The fundamental component is filtered out by the following on-chip SIW antenna which is based on metamaterial slots having high-pass characteristic.

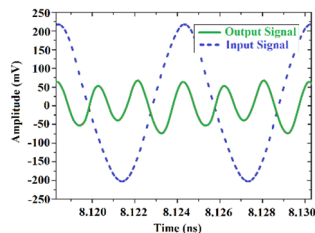


Fig.4. Simulated time-domain waveform of the frequency tripler.

### E. On-Chip Antenna Based on Substrate Integrated Waveguide and Metamaterial Slots

The proposed on-chip metamaterial slotted antenna design is based on SIW structure [9, 10]. The on-chip integrated antenna in Fig.5 consists of a SIW, a  $4 \times 4$  radiation longitudinal and transverse slot arrays, and an interconnect between a microstrip line and a SIW. The ceiling and floor of the SIW are fabricated employing the  $0.1\mu\text{m}$  aluminium pad layer and  $0.5\mu\text{m}$  GaAs layer with  $\epsilon_r$ : 12.94 and  $\tan\delta$ : 0.006, respectively. The floor of the SIW is extended to be a full ground-plane of the microstrip line. The sidewalls of a SIW structure are formed using metallic via holes from the GaAs layer to the aluminium pad layer, and the radiation longitudinal and transverse slot arrays have etched out in the pad layer based on metamaterial concept [11-14] to improve the radiation performance parameters. The gap between the end of SIW and slot arrays is set as three-quarter wavelength due to the PCB fabrication limitation. One-quarter wavelength, which can be accurately fabricated on chip, is chosen here to save the antenna footprint and enhance the radiation of the slot.

Dimensions of the SIW on-chip antenna, ground-plane, diameter of via holes, distance between via holes, length & width of slots, distance between the slots in each row, length & width of microstrip line, length & width of interconnect line are  $2 \times 1.5 \times 0.0001 \text{ mm}^3$ ,  $2 \times 2 \times 0.0005 \text{ mm}^3$ ,  $0.025 \text{ mm}$ ,  $0.077 \text{ mm}$ ,  $3 \text{ mm}$  &  $1 \text{ mm}$ ,  $3 \text{ mm}$ ,  $0.3 \text{ mm}$  &  $0.2 \text{ mm}$ ,  $0.2 \text{ mm}$  &  $0.070 \text{ mm}$ , respectively.

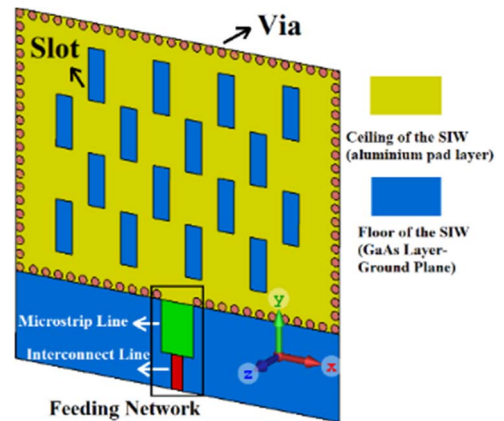


Fig.5. Configuration of the proposed on-chip antenna based on SIW and metamaterial technologies.

A SIW is used here as a high-pass structure [9] to filter out the unwanted  $f_0$  and  $2f_0$  signals. In addition, the SIW is close to waveguide structure that greatly reduces undesired surface waves and electromagnetic interference

to nearby active circuits. Finally, the input impedance of the SIW on-chip antenna can be controlled by the widths of the integrated waveguide and the microstrip line. Hence, the proposed antenna is easily conjugate matched with a tripler to minimize the loss. In addition, to increase the radiation properties of the SIW on-chip antenna, a 4×4 array of longitudinal and transverse slots were added on top of the SIW. This approach extends the effective aperture area of the on-chip antenna to optimise radiation performances.

Fig.6 shows the on-chip antenna operates over a frequency range from 300 GHz to 310 GHz.

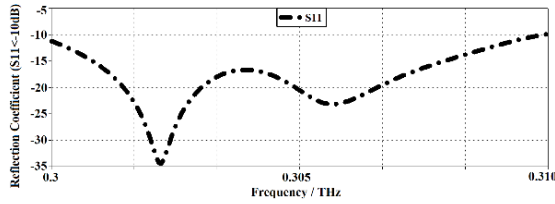


Fig.6. Reflection coefficient ( $S_{11} < -10\text{dB}$ ) of the proposed metamaterial on-chip antenna implemented on SIW.

The radiation performance parameters such as gain and efficiency plots are shown in Figs. 7 and 8. The minimum and maximum radiation gain and efficiency are 0.25 dBi at 300 GHz & 1.75 dBi at 305 GHz, and 46.12% at 310 GHz & 68.34% at ~305 GHz, respectively. The average value of these parameters are 1.05 dBi and 54.69%, respectively.

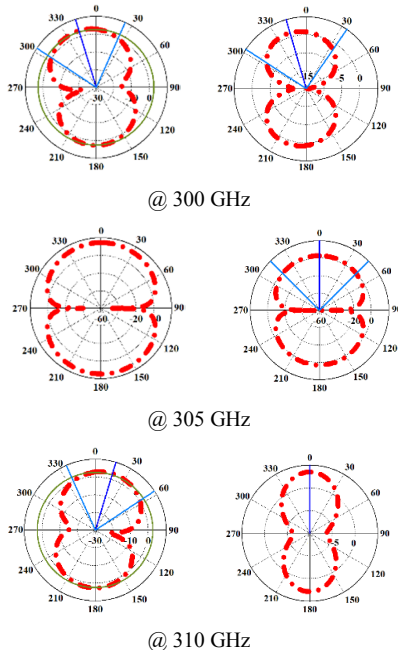


Fig.7. Radiation patterns of the proposed on-chip antenna at 300, 305, and 310 GHz. Left- and right-side show the E- and H-planes, respectively.

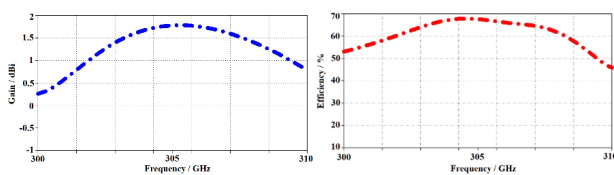


Fig.8. Radiation gain and efficiency curves of the on-chip antenna versus operational frequency.

### III. CONCLUSION

An on-chip antenna which is fully integrated on GaAs based transceiver operates across 0.3-0.31 THz. The transceiver is constructed from a voltage-controller oscillator, a buffer, a modulator, a power amplifier, a frequency tripler, and an on-chip antenna. The on-chip antenna design was constructed using SIW technology and comprises 4×4 longitudinal and transverse array slots that are realized by metamaterial technology. The on-chip antenna has a minimum gain and efficiency of 0.25 dBi and 46.12%, respectively, over 300 GHz to 310 GHz, which enable it to be applicable for near-field active imaging applications at terahertz.

### ACKNOWLEDGMENTS

This work is partially supported by innovation programme under grant agreement H2020-MSCA-ITN-2016 SECRET-722424 and the financial support from the UK EPSRC under grant EP/E022936/1.

### REFERENCES

- [1] P. D. Maagt, P. H. Bolivar, and C. Mann, "Terahertz Science, Engineering and Systems – from Space to Earth Applications," in Encyclopedia of RF and Microwave Engineering, K. Chang, Ed. Wiley, 2005, pp. 5175–5194.
- [2] M. Tonouchi, "Cutting-edge terahertz technology," Nature Photonics, vol. 1, pp. 97-105, Feb. 2007.
- [3] A. Maestrini, J. S. Ward, J. J. Gill, C. Lee, B. Thomas, R. H. Lin, G. Chattopadhyay, and I. Mehdiand, "A frequency-multiplied source with more than 1mW of power across the 840-900-GHz band," IEEE Trans. Microw. Theory Tech., vol. 58, no. 7, pp. 3477-3490, Jul. 2010.
- [4] K.B. Cooper, R.J.Dengler, N.Llombart, T. Bryllert, G. Chattopadhyay, E. Schlecht, J. Gill, C. Lee, A. Skalare, I. Mehdi, and P.H.Siegel, "Penetrating 3-D imaging at 4- and 25-m range using a submillimetre-wave radar," IEEE Trans. Microw. Theory Tech., vol. 56, no. 12, pp. 2771-2778, Dec. 2008.
- [5] E. Laskin, M. Khanpour, S. T. Nicolson, A. Tomkins, P. Garcia, A. Cathelin, D. Belot, and S. P. Voinigescu, "Nanoscale CMOS transceiver design in the 90-170-GHz range," IEEE Trans. Microw. Theory Tech., vol. 57, no. 12, pp. 3477-3490, Dec. 2009.
- [6] B. Razavi, "A 300-GHz fundamental receiver for automotive radar," IEEE J. Solid-State Circuits, vol. 46, no. 4, pp. 894-903, Apr. 2011.
- [7] E. Seok et al., "Progress and challenges towards terahertz CMOS integrated circuits," IEEE J. Solid-State Circuits, vol. 45, no. 8, pp. 1554-1564, Aug. 2010.
- [8] E. Öjefors, J. Grzyb, Y. Zhao, B. Heinemann, B. Tillack, and U. R. Pfeiffer, "A 820GHz SiGe chipset for terahertz active imaging applications," ISSCC Dig. Tech. Papers, pp. 224-225, Feb. 2011.
- [9] D. Deslandes and K. Wu, "Accurate modeling, wave mechanisms, and design considerations of a substrate integrated waveguide," IEEE Trans. Microw. Theory Tech., vol. 54, no. 6, pp. 2516-2525, 2006.
- [10] L. Yan, W. Hong, G. Hua, J. Chen, K. Wu, and T. J. Cui, "Simulation and experiment on SIW slot array antennas," IEEE Microw. Wireless Compon. Lett., vol. 14, no. 9, pp. 446-448, 2004.
- [11] M. Alibakhshi-Kenari, M. Naser-Moghadasi, R. A. Sadeghzadeh, B. S. Virdee and E. Limiti, "Periodic Array of Complementary Artificial Magnetic Conductor Metamaterials-Based Multiband Antennas for Broadband Wireless Transceivers," IET Microwaves, Antennas & Propagation, vol.10, issue 15, 10 December 2016, pp.1682 – 1691.
- [12] M. Alibakhshi-Kenari, M. Naser-Moghadasi, R. A. Sadeghzadeh, B. S. Virdee and E. Limiti, "Bandwidth Extension of Planar Antennas Using Embedded Slits for Reliable Multiband RF Communications", AEUE Elsevier-International Journal of Electronics and Communications, vol.70, issue 7, July 2016, pp. 910–919.
- [13] R. A. Sadeghzadeh, M. Alibakhshi-Kenari and M. Naser-Moghadasi, "UWB Antenna Based on SCRLH-TLs for Portable Wireless Devices", Microwave and Optical Technology Letters, vol.58, issue 1, January 2016, pp.69–71.
- [14] M. Alibakhshi-Kenari, A. Andújar and J. Anguera, "New Compact Printed Leaky-Wave Antenna with Beam Steering," Microwave and Optical Technology Letters, vol.58, issue 1, January 2016, pp. 215–217.